High-accuracy zenith delay prediction at optical wavelengths

V. B. Mendes

Laboratório de Tectonofísica e Tectónica Experimental and Departamento de Matemática, Faculdade de Ciências da Universidade de Lisboa, Lisbon, Portugal

E. C. Pavlis

Joint Center for Earth Systems Technology, University of Maryland Baltimore County and NASA Goddard Space Flight Center, Greenbelt, Maryland, USA

Received 20 April 2004; revised 9 June 2004; accepted 16 June 2004; published 16 July 2004.

[1] A major limitation in accuracy in modern satellite laser ranging is the modeling of atmospheric refraction. Recent improvements in this area include the development of mapping functions to project the atmospheric delay experienced in the zenith direction to a given elevation angle. In this paper, we derive zenith delay models from revised equations for the computation of the refractive index of the atmosphere, valid for a wide spectrum of optical wavelengths. The zenith total delay predicted with these models were tested against ray tracing through radiosonde data from a full year of data, for 180 stations distributed worldwide, and showed sub-millimeter accuracy for wavelengths ranging from 0.355 μm to 1.064 μm. *INDEX TERMS:* 1243 Geodesy and Gravity: Space geodetic surveys; 1294 Geodesy and Gravity: Instruments and techniques; 6904 Radio Science: Atmospheric propagation. **Citation:** Mendes, V. B., and E. C. Pavlis (2004), High-accuracy zenith delay prediction at optical wavelengths, *Geophys. Res. Lett.*, *31*, L14602, doi:10.1029/2004GL020308.

1. Introduction

[2] The accuracy of satellite laser ranging (SLR) is greatly affected by the residual errors in modeling the effect of signal propagation through the troposphere and stratosphere. Although several models for atmospheric correction have been developed, the more traditional approach in SLR data analysis uses a model developed in the 1970s [*Marini and Murray*, 1973] (the correction of the atmospheric delay using two-color ranging systems is still at an experimental stage). A recent study [*Mendes et al.*, 2002] points out some limitations in that model, namely as regards the modeling of the elevation dependency of the zenith atmospheric delay (the mapping function (MF) component of the model). The MFs developed by *Mendes et al.* [2002] represent a significant improvement over the MF built-in in the Marini-Murray model and other known MFs. Of particular interest is the ability of the new MFs to be used in combination with any zenith delay (ZD) model, used to predict the atmospheric delay in the zenith direction. The next logical step is the development of more accurate ZD models applicable to the range of wavelengths used in modern SLR instrumentation.

2. Group Refractivity

[3] The atmospheric propagation delay experienced by a laser signal in the zenith direction is defined as

$$d^z_{atm} = 10^{-6} \int_{r_s}^{r_a} N dz = \int_{r_s}^{r_a} (n-1) dz, \tag{1}$$

or, if we split the ZD into a hydrostatic (d^z_h) and a non-hydrostatic (d^z_{nh}) components,

$$d^z_{atm} = d^z_h + d^z_{nh} = 10^{-6} \int_{r_s}^{r_a} N_h dz + 10^{-6} \int_{r_s}^{r_a} N_{nh} dz, \tag{2}$$

where $N = (n - 1) \times 10^6$ is the (total) group refractivity of moist air, n is the (total) refractive index of moist air, N_h and N_{nh} are the hydrostatic and the non-hydrostatic components of the refractivity, r_s is the geocentric radius of the laser station, r_a is the geocentric radius of the top of the (neutral) atmosphere, and dz has length units.

[4] Following the recommendations of the International Association of Geodesy (IAG) [*International Union of Geodesy and Geophysics* (*IUGG*), 1999] the group refractivity for visible and near-infrared waves should be computed using the procedures described by *Ciddor* [1996] and *Ciddor and Hill* [1999]. The formula for the computation of the refractivity is [*Ciddor*, 1996]:

$$N = \left(\frac{\rho_a}{\rho_{axs}}\right) N_{gaxs} + \left(\frac{\rho_w}{\rho_{ws}}\right) N_{gws}, \tag{3}$$

where ρ_a is the density of dry air component for actual conditions (kg m^{-3}), ρ_w is the density of water vapor (WV) component for actual conditions (kg m^{-3}), ρ_{axs} is the density of (standard) dry air at 15°C, 101325 Pa, and $x_w = 0$ (where $x_w = e/P$ is the molar fraction of WV in moist air (unitless), e is the WV pressure of moist air (Pa), and P is the total pressure (Pa)), and ρ_{ws} is the density of (standard) pure WV at 20°C, 1333 Pa, and $x_w = 1$.

[5] The group refractive index for the dry air component (unitless), N_{gaxs}, is given by [*Ciddor*, 1996]:

$$N_{gaxs} = 10^{-2} \left[k_1 \frac{(k_0 + \sigma^2)}{(k_0 - \sigma^2)^2} + k_3 \frac{(k_2 + \sigma^2)}{(k_2 - \sigma^2)^2} \right] C_{CO_2}, \tag{4}$$

0094-8276/04/2004GL020308$05.00

where k_0 = 238.0185 μm^{-2}, k_1 = 5792105 μm^{-2}, k_2 = 57.362 μm^{-2}, k_3 = 167917 μm^{-2} (see the auxiliary material[1]), σ is the wave number ($\sigma = \lambda^{-1}$, where λ is the vacuum wavelength, in μm), $C_{CO2} = 1 + 0.534 \times 10^{-6}$ $(x_c - 450)$, and x_c is the carbon dioxide (CO_2) content, in ppm (in this paper we will always assume a CO_2 content of 375 ppm, in line with the IAG recommendations).

[6] The group refractive index for the WV component (unitless), N_{gws}, is [*Ciddor*, 1996]:

$$N_{gws} = 10^{-2} cf\left(\omega_0 + 3\omega_1\sigma^2 + 5\omega_2\sigma^4 + 7\omega_3\sigma^6\right), \tag{5}$$

where cf is a correction factor (cf = 1.022), ω_0 = 295.235, ω_1 = 2.6422 μm^2, ω_2 = −0.032380 μm^4, and ω_3 = 0.004028 μm^6.

[7] Furthermore, we have:

$$\rho_a = \frac{PM_d(1 - x_w)}{ZRT}, \tag{6}$$

where M_d is the molar mass of dry air containing x_c ppm of CO_2 (that is, M_d = 0.0289632 kg mol^{-1}), R is the universal gas constant (R = 8.314510 J mol^{-1} K^{-1}), T is the temperature, in Kelvin ($T = t + 273.15$, where t is the temperature, in °C), and Z is the compressibility factor of moist air,

$$Z = 1 - \left(\frac{P}{T}\right)\left\{a_0 + a_1 t + a_2 t^2 + (b_0 + b_1 t)x_w + (c_0 + c_1 t)x_w^2\right\} + \left(\frac{P}{T}\right)^2\left(d_0 + e_0 x_w^2\right) \tag{7}$$

with $a_0 = 1.58123 \times 10^{-6}$ K Pa^{-1}, $a_1 = -2.9331 \times 10^{-8}$ Pa^{-1}, $a_2 = 1.1043 \times 10^{-10}$ K^{-1} Pa^{-1}, $b_0 = 5.707 \times 10^{-6}$ K Pa^{-1}, $b_1 = -2.051 \times 10^{-8}$ Pa^{-1}, $c_0 = 1.9898 \times 10^{-4}$ K Pa^{-1}, $c_1 = -2.376 \times 10^{-6}$ Pa^{-1}, $d_0 = 1.83 \times 10^{-11}$ K^2 Pa^{-2}, and $e_0 = -0.765 \times 10^{-8}$ K^2 Pa^{-2}.

[8] The density of standard dry air, ρ_{axs}, is computed using equation (6) with P_d = 101325 Pa, T_d = 288.15 K, and x_w = 0:

$$\rho_{axs} = \frac{P_d M_d}{Z_d R T_d}, \tag{8}$$

and the compressibility factor of dry air, Z_d, is computed using equation (7) for same standard conditions, that is,

$$Z_d = 1 - \left(\frac{P_d}{T_d}\right)\left(a_0 + a_1 t_d + a_2 t_d^2\right) + \left(\frac{P_d}{T_d}\right)^2 d_0, \tag{9}$$

where t_d = 15°C.

[9] Similarly, we have for the density of the WV component of moist air:

$$\rho_w = \frac{PM_w x_w}{ZRT}, \tag{10}$$

where M_w is the molar mass of WV (M_w = 0.018015 kg mol^{-1}).

[10] Finally we compute the density of pure WV at standard conditions, ρ_{ws}, using equation (10) with P_w = 1333 Pa, T_w = 293.15 K, and x_w = 1:

$$\rho_{ws} = \frac{P_w M_w}{Z_w R T_w}, \tag{11}$$

[1]Auxiliary material is available at ftp://ftp.agu.org/apend/gl/2004GL020308.

and the corresponding compressibility factor, Z_w, computed for the same conditions,

$$Z_w = 1 - \left(\frac{P_w}{T_w}\right)\{a_0 + a_1 t_w + a_2 t_w^2 + (b_0 + b_1 t_w) + (c_0 + c_1 t_w)\} + \left(\frac{P_w}{T_w}\right)^2 (d_0 + e_0), \tag{12}$$

where t_w = 20°C.

3. Zenith Hydrostatic Delay

[11] To derive an expression for the zenith hydrostatic delay, we start by computing

$$\frac{\rho_a}{\rho_{axs}} = \left(\frac{T_d}{P_d}\right)\left(\frac{Z_d}{Z}\right)\left(\frac{P}{T}\right) - \left(\frac{T_d}{P_d}\right)\left(\frac{Z_d}{Z}\right)\left(\frac{e}{T}\right). \tag{13}$$

[12] As the density of moist air ρ is [*Ciddor*, 1996]

$$\rho = \frac{M_d}{ZR}\left[\frac{P}{T} - (1 - \varepsilon)\frac{e}{T}\right], \tag{14}$$

then,

$$\frac{P}{T} = Z\rho R_d + (1 - \varepsilon)\frac{e}{T}, \tag{15}$$

where $R_d = R/M_d$ is the mean specific gas constant for dry air (R_d = 287.07153 J kg^{-1} K^{-1}) and $\varepsilon = \frac{M_w}{M_d}$.

[13] Given that, we obtain:

$$\frac{\rho_a}{\rho_{axs}} = \left(\frac{T_d}{P_d}\right) Z_d \rho R_d - \varepsilon\left(\frac{T_d}{P_d}\right)\left(\frac{Z_d}{Z}\right)\left(\frac{e}{T}\right). \tag{16}$$

[14] For the computation of the hydrostatic component of group refractivity we will use only the first term of the right hand-side of equation (16), as the second term depends on the WV pressure. Therefore,

$$N_h = N_{gaxs}\left(\frac{T_d}{P_d}\right) Z_d \rho R_d. \tag{17}$$

[15] In modern SLR systems, the most commonly used wavelength is λ = 0.532 μm. The group refractivity for the dry air component for this particular wavelength, here denominated as N_{gaxs}^{532}, is computed using equation (4) and we have $N_{gaxs}^{532} = 10^6 \times (n_{gaxs}^{532} - 1) \approx 289.736$.

[16] As a result, we can simplify equation (17):

$$N_h = 289.736\, f_h(\lambda)\left(\frac{T_d}{P_d}\right) Z_d \rho R_d, \tag{18}$$

or,

$$N_h = K_1^L\, f_h(\lambda) Z_d \rho R_d, \tag{19}$$

where K_1^L = 0.8239568 K Pa^{-1}, and the modified group refractivity for dry air, $f_h(\lambda)$, is our dispersion equation for the hydrostatic component,

$$f_h(\lambda) = 10^{-2}\left[k_1^* \frac{(k_0 + \sigma^2)}{(k_0 - \sigma^2)^2} + k_3^* \frac{(k_2 + \sigma^2)}{(k_2 - \sigma^2)^2}\right] C_{CO_2}, \tag{20}$$

with k_1^* = 19990.975 μm^{-2}, and k_3^* = 579.55174 μm^{-2}.

[17] The zenith hydrostatic delay is thus:

$$d_h^z = 10^{-6} K_1^L f_h(\lambda) Z_d R_d \int_{r_s}^{r_a} \rho dz \tag{21}$$

[18] Using the hydrostatic equation, we get

$$\int_{r_s}^{r_a} \rho dz = -\int_{P_s}^{0} \frac{dP}{g} = \frac{P_s}{g_m}, \tag{22}$$

where P_s is the surface barometric pressure (Pa), and g_m is the acceleration due to gravity at the center of mass of the vertical column of air (m s^{-2}) [*Saastamoinen*, 1973],

$$g_m = 9.784\, f(\varphi, H), \tag{23}$$

$$f(\varphi, H) = 1 - 0.00266 \cos 2\varphi - 0.00028H, \tag{24}$$

φ is the latitude of the station, and H is the height of the station, in km. Replacing equation (22) into equation (21) leads to

$$d_h^z = 10^{-6} K_1^L f_h(\lambda) Z_d R_d \frac{P_s}{g_m}. \tag{25}$$

Replacing the known constants, we get the final expression for the *zenith hydrostatic delay*, in meter units,

$$d_h^z = 0.00002416579 \frac{f_h(\lambda)}{f(\varphi, H)} P_s. \tag{26}$$

4. Zenith Non-Hydrostatic Delay

[19] The first non-hydrostatic component of the group refractivity, N_{nh1}, arises from the second term of the right hand-side of equation (16):

$$N_{nh1} = -N_{gaxs} \left(\frac{T_d}{P_d}\right) \left(\frac{Z_d}{Z}\right) \left(\frac{e}{T}\right) \varepsilon \tag{27}$$

or, following the previous development,

$$N_{nh1} = -K_L^1 \varepsilon f_h(\lambda) \left(\frac{Z_d}{Z}\right) \left(\frac{e}{T}\right). \tag{28}$$

The second non-hydrostatic component is given as:

$$N_{nh2} = N_{gws} \left(\frac{\rho_w}{\rho_{ws}}\right), \tag{29}$$

and

$$\frac{\rho_w}{\rho_{ws}} = \left(\frac{T_w}{P_w}\right) \left(\frac{Z_w}{Z}\right) \left(\frac{e}{T}\right). \tag{30}$$

[20] For λ = 0.532 µm we get $N_{gws}^{532} \approx 3.2956$, hence

$$N_{nh2} = 3.2956 f_{nh}(\lambda) \left(\frac{T_w}{P_w}\right) \left(\frac{Z_w}{Z}\right) \left(\frac{e}{T}\right), \tag{31}$$

where the dispersion formula for the non-hydrostatic component is

$$f_{nh}(\lambda) = 0.003101 \left(\omega_0 + 3\omega_1 \sigma^2 + 5\omega_2 \sigma^4 + 7\omega_3 \sigma^6\right) \tag{32}$$

that is,

$$N_{nh2} = K_2^L f_{nh}(\lambda) \left(\frac{Z_w}{Z}\right) \left(\frac{e}{T}\right), \tag{33}$$

with K_2^L = 0.7247600 K Pa^{-1}.

[21] The non-hydrostatic component of group refractivity is therefore computed from the contribution arising from equation (28) and equation (33):

$$N_{nh} = -K_1^L \varepsilon f_h(\lambda) \left(\frac{Z_d}{Z}\right) \left(\frac{e}{T}\right) + K_2^L f_{nh}(\lambda) \left(\frac{Z_w}{Z}\right) \left(\frac{e}{T}\right). \tag{34}$$

[22] As the ratio between compressibility factors can be safely ignored, the zenith non-hydrostatic delay is thus:

$$d_{nh}^z = 10^{-6} \left(K_2^L f_{nh}(\lambda) - K_1^L \varepsilon f_h(\lambda)\right) \int_{r_s}^{r_a} \frac{e}{T} dz. \tag{35}$$

[23] For the computation of the integral in equation (35), we can use the following approximation [*Saastamoinen*, 1973]:

$$\int_{r_s}^{r_a} \frac{e}{T} dz \doteq \frac{R_d}{\nu g_m} e_s, \tag{36}$$

where ν is a numerical coefficient to be determined from local observations (average value $\nu = 4$) and e_s is the surface water vapor pressure (the coefficient ν is highly variable in space and time and should be chosen to fit the location and season, for maximum accuracy in the determination of the non-hydrostatic component). As a result, we have

$$d_{nh}^z = 10^{-6} \left(K_2^L f_{nh}(\lambda) - K_1^L \varepsilon f_h(\lambda)\right) \frac{\mathrm{R_d}}{\nu \mathrm{g_m}} \mathrm{e_s}, \tag{37}$$

or, after replacing for the known constants, we get the expression for the *zenith non-hydrostatic delay*:

$$d_{nh}^z = 10^{-6} (5.316 f_{nh}(\lambda) - 3.759 f_h(\lambda)) \frac{\mathrm{e_s}}{f(\varphi, H)}. \tag{38}$$

5. Experimental Validation

[24] In order to assess the performance of the derived ZD models, we performed a comparison against ray tracing of radiosonde data, for 180 stations [see *Mendes et al.*, 2002] with typically two balloon launches per day, a full year of data (1998), and for the most used wavelengths in SLR:

0.355, 0.423, 0.532, 0.6943, 0.847, and 1.064 μm. The ray tracing was performed using the full formulation of the group refractivity given by *Ciddor* [1996]. We have also included in this assessment the ZD models developed by *Saastamoinen* [1973] and *Marini and Murray* [1973]. The surface meteorological parameters needed to drive the different models are obtained directly from the radiosonde data. Due to the different strategies in splitting the ZD into its hydrostatic and non-hydrostatic components, the analysis is performed only for the total delay. For discussion purposes, the model developed in this paper (sum of the contribution of the hydrostatic and non-hydrostatic component) will be labeled FCULzd.

[25] The results of this assessment are summarized in Table 1. The statistics represent the mean, standard deviation (std), and root-mean-square (rms) for the total number of differences between the predictions given by the models and the ray tracing benchmark values (model minus tracing). From this table, it can be concluded that the differences in performance of the models are essentially in the bias component, as the standard deviation of the differences is very similar to all models (and below the 1-mm level). For wavelengths greater than 0.532 μm the mean biases for the Saastamoinen (SAAS) and Marini-Murray (MM) models are at the 1-mm level, indicating an overprediction of the ZD. The MM model has a very small negative bias at the 0.423 μm wavelength, but this bias increases significantly for lower wavelengths, showing therefore a variable behavior. In the case of the SAAS model, there is an underprediction of more than 7 mm at the 0.355 μm wavelength. The FCULzd model is essentially non-biased and present identical or better standard deviations at all wavelengths, despite the small trend of increase towards the lower wavelengths. The overall rms values for the total zenith delay are below 1 mm across the whole wavelength spectrum analyzed.

[26] When compared against the MM model, the advantage of the FCULzd model in reducing the bias is clearly seen in the box-and-whisker plots shown in Figure 1 (for the sake of clarity, the values at 0.355 μm were excluded, due to the large biases for the MM model). We can conclude from these plots that the percentage of stations where the rms for FCULzd exceeds 1 mm rms is below 10 percent, for wavelengths larger than 0.532 μm. The maximum rms value observed is of 2.0 mm (station Seychelles), for the 0.355 μm wavelength. These higher values are generally associated with stations with large water vapor content, such as those located in the equatorial regions and Southwest Pacific and may therefore be associated with the non-hydrostatic component of the ZD. One of the reasons may be the use of a fixed value for ν. This fact is also likely responsible for the slight but consistently negative mean bias for FCULzd. As regards the MM model, a bias of more than 1 mm is clear at all wavelengths greater than 0.423 μm (this bias was already noted by *Mendes et al.* [2002]; note that, due to a typo, the units in Table 3 of *Mendes et al.* [2002] are wrongly labeled with cm instead of mm). That bias is below 1-mm at 0.423 μm, but even at this wavelength the number of stations with rms values greater than 1 mm is near 25 percent. Furthermore the anomalous behavior of the MM model across the whole wavelength spectrum used in SLR constitutes a serious handicap in combining solutions obtained with different systems.

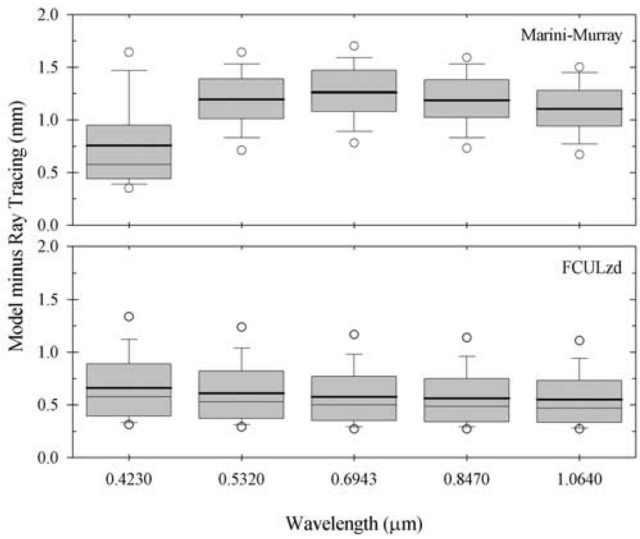

Figure 1. Box-and-whisker plots for the FCULzd and Marini-Murray zenith delay models using the rms values obtained at each individual radiosonde station. The statistical quantities represented are the median and the mean (thinner and thicker lines inside the boxes, respectively), the 25th and 75th percentiles (vertical box limits), the 10th and 90th percentiles (whiskers), and the 5th and 95th percentiles (open circles).

Table 1. Statistics for the Zenith Delay Differences With Respect to Ray Tracing (Model Minus Ray Tracing)

λ (μm)	Model	Mean (mm)	Std (mm)	Rms (mm)
0.355	Marini-Murray	−4.0	1.0	4.1
	Saastamoinen	−7.4	1.0	7.5
	FCUL	−0.1	0.7	0.8
0.423	Marini-Murray	−0.2	0.8	0.8
	Saastamoinen	1.3	0.8	1.5
	FCUL	−0.1	0.7	0.7
0.532	Marini-Murray	1.0	0.7	1.2
	Saastamoinen	1.0	0.7	1.2
	FCUL	−0.1	0.6	0.6
0.6943	Marini-Murray	1.1	0.6	1.3
	Saastamoinen	1.1	0.6	1.4
	FCUL	−0.1	0.6	0.6
0.847	Marini-Murray	1.1	0.6	1.2
	Saastamoinen	1.1	0.6	1.2
	FCUL	−0.1	0.6	0.6
1.064	Marini-Murray	1.0	0.6	1.1
	Saastamoinen	0.8	0.6	1.0
	FCUL	−0.1	0.6	0.6

[27] In summary, we have developed a new zenith delay model that is based on up-to-date formulae to compute the refractivity at visible and near-infrared wavelengths, that can be combined with state-of-the-art mapping functions to model more accurately the atmospheric refraction for the full wavelength spectrum used in SLR.

[28] **Acknowledgments.** E. C. Pavlis gratefully acknowledges partial support of this project from NASA's Cooperative Agreement NCC5-339 and the NURI Grant NMA201-01-BAA-2002. Radiosonde data were kindly provided by the British Atmospheric Data Center (BADC). The ray-trace software was developed by James Davis, Thomas Herring, and Arthur Niell. The authors would like to thank the Refraction Study Group

of the International Laser Ranging Service for fruitful discussions and to Pedro Elósegui for valuable comments on the manuscript.

References

Ciddor, P. E. (1996), Refractive index of air: New equations for the visible and near infrared, *Appl. Opt.*, *35*, 1566–1573.

Ciddor, P. E., and R. J. Hill (1999), Refractive index of air. 2. Group index, *Appl. Opt.*, *38*, 1663–1667.

International Union of Geodesy and Geophysics (IUGG) (1999), Resolution 3 of the International Association of Geodesy, in *Comptes Rendus of the XXII General Assembly*, pp. 110–111, Birmingham, UK.

Marini, J. W., and C. W. Murray (1973), Correction of laser range tracking data for atmospheric refraction at elevations above 10 degrees, *NASA Tech. Memo., NASA-TM-X-70555*, 60 pp.

Mendes, V. B., G. Prates, E. C. Pavlis, D. E. Pavlis, and R. B. Langley (2002), Improved mapping functions for atmospheric refraction correction in SLR, *Geophys. Res. Lett.*, *29*(10), 1414, doi:10.1029/2001GL014394.

Saastamoinen, J. (1973), Contributions to the theory of atmospheric refraction, part II, Refraction corrections in satellite geodesy, *Bull. Geod.*, *107*, 13–24.

V. B. Mendes, Departamento de Matemática, Faculdade de Ciências da Universidade de Lisboa, P-1749-016 Lisboa, Portugal. (vmendes@fc.ul.pt)

E. C. Pavlis, Joint Center for Earth Systems Technology, University of Maryland Baltimore County and NASA Goddard 926, Greenbelt, MD 20771, USA. (epavlis@jcet.umbc.edu)